A 3D BiCG Iterative Solver with the Fourier Preconditioner for the Anisotropic EIT / EEG forward problem

Sergei Turovets[1, 3], Vasily Volkov[2], Aleksej Zherdetsky[2], Elena Prokonina[2] and Allen Malony[3]

[1]Electrical Geodesics, Inc., Eugene, OR 97403, USA
[2]Department of Mathematics and Mechanics, Belarusian State University, Minsk 220050, Republic of Belarus
[3]NeuroInformatics Center, 5294 University of Oregon, Eugene, OR 97403, USA
e-mail: sergei@cs.uoregon.edu ; volkovvm@bsu.by

Abstract

The EIT/EEG forward solution in anisotropic inhomogeneous media like head tissues belongs to the class of the three-dimensional boundary value problems for elliptic equations with mixed derivatives. The proposed numerical scheme is based on the finite-difference approximation of the corresponding discrete problem for the anisotropic inhomogeneous Poisson equation in an arbitrary three-dimensional computational domain, augmented to a cuboid with non-conducting claddings and the boundary conditions defined at the facets of the cuboid (the Dirichlet type). The rectangular uniform finite difference grid is assumed to have high enough resolution across the characteristic layers of inhomogeneity. The nonconductive claddings imitate the Neumann boundary condition on the arbitrarily shaped surface of the embedded object. The discrete problem is reduced to solving a system of linear algebraic equations with a 19-diagonal sparse matrix. Use of iterative methods from the BiCG family is most effective with the adequate choice of preconditioners. As a preconditioner in this problem, we have employed an analog of the finite difference operator of the corresponding discrete problem with constant coefficients (the homogeneous problem). This type of preconditioning is known as the Fourier-Laplace (FL) preconditioning and it is an option of choice due to the relative similarity of the eigenvalues spectral characteristics for the homogeneous and inhomogeneous discrete problems. Also, the method is attractive due to the possibility of matrix diagonalization with the discrete fast Fourier transform. The proposed algorithm has been validated against analytics in a spherical model and tested on the anatomically accurate MRI based human head geometry and showed high efficiency. The FL type preconditioner in the BiCG method allowed to reduce the number of iterations to convergence by factor of several dozens. Furthermore, in this case it is possible to model extremely high heterogenity including metal surgical clips and implants and eliminate the characteristic increase in the number of iterations with the increase of resolution of the discrete problem. Overall, the proposed technique is comparable with efficiency of the multigrid finite difference iterative methods.

1 Introduction

The progress in forward and inverse modeling in Electrical Encephalography (EEG) source localization and Electrical Impedance Tomography (EIT) depends on the efficiency and accuracy of the employed forward solvers for the governing partial differential equation (PDE) , the Poisson equation, describing the volume conduction in highly heterogeneous and anisotropic human head tissues.

The modern forward solvers use the variety of computational approaches based on the finite difference, boundary element and finite element methods [1-3], multigrid [17] and preconditioned CG-type iterative methods [15,16, 18] and also high performance parallel computing techniques [4,6,20, 21].

Previously, we built an iterative finite difference forward problem solver for an isotropic version of the Poisson equation for EEG/EIT based on the multi-component alternating directions implicit (ADI) algorithm [6]. It is a generalization of the classic ADI algorithm, but with improved stability in 3D (the multi-component FD ADI scheme is unconditionally stable in 3D for any value of the time step [7,8]). To describe the electrical conductivity in the heterogeneous biological media within arbitrary geometry, the method of embedded boundaries or a fictitious domain has been used [14]. Here an object of interest is embedded into a cubic computational domain with extremely low conductivity values in the external complimentary regions modeling the surrounding air. This effectively guarantees there are no current flows out of the physical area. The idea of the iterative implicit method is to find the solution as a steady state of the appropriate evolution (diffusion) problem. At every iteration step, the spatial operator is split into the sum of three 1D operators, which are evaluated alternatively at each sub-step. Such a scheme is accurate to $O[\tau +(\Delta x)^2)+(\Delta y)^2+(\Delta z)^2]$. In contrast with the classic ADI method, the multi-component ADI uses the regularization (averaging) for evaluation of the variable at the previous instant of time. Parallelization of the vector-additive ADI algorithm in a shared memory multiprocessor environment (OpenMP) is straightforward, as it consists of nests of independent loops over “bars” of voxels for solving the effective 1D problem in every iteration [6]. However, the ADI method is less suitable for implementation in an environment with a distributed memory. Therefore we also presented in the past an anisotropic vector-additive algorithm [21] of the domain decomposition type [9] which is potentially amenable for implementation at greater parallel degree [4].

The methods belonging to the family of the Conjugate Gradient (CG) methods [13, 15, 17] have become the most attractive recent iterative techniques for solving the forward EEG /EIT problem. These methods have the high convergence rate to reach the required accuracy which is proportional to a square root from a condition number of a system matrix in Large Algebraic Equations (LAE). In case of a finite difference grid , a condition number of a system matrix is inversely proportional to a grid step squared resulting in increase of the iteration number with the grid resolution. Additionally, a condition number depends from the heterogeneity of coefficients in PDE, in particular , the ratio of maximal and minimal conductivities in the media. To reduce a condition number, one needs to implement preconditioned CG-type iterative methots such as BiCG [15] and BiCGStab [17] in cases of strongly heterogeneous and anisotropic conductive media. In this paper we demonstrate applicability of the finite difference method using benefits of the Fast Fourier Transform technique as a tool for building a quasy-optimal preconditioner for the CG type iterative solvers. As a quasy – optimal preconditioner we suggest the matrix of the corresponding Dirichlet problem with homogeneous isotropic coefficients in the same ficticious computational domain. In spite of this idea

is not new (see for instance [14]), for the EIT/EEG configutations it was used so far only in our previous work on the isotropic cylinder phantom EIT forward solver [16].

It is worth to note, that the spectrally quasy-optimal preconditioner based on FFT has no analogies in FEM using adaptive nonuniform grids. In addition, our FDM choice is dictated by the rectangular voxels form of the medical imaging modalities surving as input geometries in EEG/EIT and linear dependence of the FDM solution accuracy from the rectangular medical image resolution.

2 Finite-Difference Model

The relevant frequency spectrum in EEG, MEG and EIT of the human head is typically below 1 kHz, and most studies deal with frequencies between 0.1 and 100 Hz. Therefore, the physics of EEG/MEG can be well described by the quasi-static approximation of the Maxwell equations, the Poisson equation [3]. The electrical forward problem can be stated as follows: given the positions, orientations and magnitudes of dipole current sources, $\varphi(x, y, z)$, as well as geometry and electrical conductivity of the head volume (Ω), calculate the distribution of the electrical potential on the surface of the head (scalp) (Γ_ω). Mathematically, it means solving the inhomogeneous anisotropic Poisson equation [2]:

$$\nabla \bullet (\sigma \nabla u) = \varphi(x,y,z), \text{ in } \Omega \tag{1a}$$

with no-flux Neumann boundary conditions on the scalp:

$$\sigma(\nabla u) \bullet n = 0, \text{ on } \Gamma_\omega. \tag{1b}$$

Here $\sigma = \sigma_{ij}(x,y,z)$ is an inhomogeneous symmetric tensor of the head tissues conductivity. Having computed potentials u(x,y,z) and current densities $J = -\sigma(\nabla u)$, the magnetic field B can be found through the Biot-Savart law. The similar non-stationary anisotropic diffusion equation is relevant also in the DOT forward problem modeling [1], spread of tumor in brain [3] and the white matter tractography studies using diffusion tensor MRI imaging [5].

In this paper we will use finite difference approximation of the spatial derivatives on the uniform rectangular grid with a 19-point stencil made of 8 voxels with one common node, as shown in Fig. 1. All stencil nodes belong to three mutually orthogonal planes. Let us illustrate the discretization on the example of plane Oxy. For approximation of the second derivatives we have used the standard conservative scheme for the finite volumes [7,10]:

$$\frac{\partial}{\partial x}\sigma_{xx}\frac{\partial u}{\partial x} = h_x^{-2}\left[\sigma_{xx}^{02}U_2 - \left(\sigma_{xx}^{02} + \sigma_{xx}^{04}\right)U_0 + \sigma_{xx}^{04}U_4\right] + O(h_x^2), \tag{2}$$

where $\sigma_{xx}^{km} = (\sigma_{xx}^{m} + \sigma_{xx}^{k})/2$, ands indices (superscripts and subscripts) refer to conductivity parameters and potentials in corresponding stencil nodes , as shown in Fig. 1. For approximation of the mixed derivatives we have investigated five kinds of the second order accuracy schemes. As an example we present here these approximations only for one of the mixed derivatives:

A. $$\frac{\partial}{\partial x}\sigma_{xy}\frac{\partial u}{\partial y}=\frac{1}{4h_yh_x}\Big(\sigma_{xy}^{2}(U_6-U_2)-\sigma_{xy}^{0}(U_3-U_0)+\sigma_{xy}^{0}(U_0-U_1)-\sigma_{xy}^{4}(U_4-U_8)+$$
$$\sigma_{xy}^{2}(U_2-U_5)-\sigma_{xy}^{0}(U_0-U_1)+\sigma_{xy}^{0}(U_3-U_0)-\sigma_{xy}^{4}(U_7-U_4)\Big)+O(h_x^2+h_y^2),$$

B. $$\frac{\partial}{\partial x}\sigma_{xy}\frac{\partial u}{\partial y}=\frac{1}{4h_yh_x}\Big(\sigma_{xy}^{+2}(U_6-U_2)-\sigma_{xy}^{+0}(U_3-U_0)+\sigma_{xy}^{+0}(U_0-U_1)-\sigma_{xy}^{+4}(U_4-U_8)+$$
$$\sigma_{xy}^{-2}(U_2-U_5)-\sigma_{xy}^{-0}(U_0-U_1)+\sigma_{xy}^{-0}(U_3-U_0)-\sigma_{xy}^{-4}(U_7-U_4)\Big)+O(h_x^2+h_y^2),$$

C. $$\frac{\partial}{\partial x}\sigma_{xy}\frac{\partial u}{\partial y}=\frac{1}{4h_yh_x}\Big(\sigma_{xy}^{26}(U_6-U_2)-\sigma_{xy}^{03}(U_3-U_0)+\sigma_{xy}^{01}(U_0-U_1)-\sigma_{xy}^{48}(U_4-U_8)+$$
$$\sigma_{xy}^{25}(U_2-U_5)-\sigma_{xy}^{01}(U_0-U_1)+\sigma_{xy}^{03}(U_3-U_0)-\sigma_{xy}^{47}(U_7-U_4)\Big)+O(h_x^2+h_y^2),\qquad(3)$$

D. $$\frac{\partial}{\partial x}\sigma_{xy}\frac{\partial u}{\partial y}=\frac{1}{4h_yh_x}\Big(\sigma_{xy}^{2}(U_6-U_5)-\sigma_{xy}^{4}(U_7-U_8)\Big)+O(h_x^2+h_y^2).$$

E. $$\frac{\partial}{\partial x}\sigma_{xy}\frac{\partial u}{\partial y}=\frac{1}{4h_yh_x}\Big(\sigma_{xy}^{02}(U_6-U_5+U_3-U_1)-\sigma_{xy}^{04}(U_3-U_1+U_7-U_8)\Big)+O(h_x^2+h_y^2),$$

where $\sigma_{xy}^{\pm k}=\sigma_{xy}^{k}\pm\left|\sigma_{xy}^{k}\right|$. One can see that in the homogeneous case of constant conductivity all of these approximations (except the case (3B)) are equivalent. In the case of inhomogeneous anisotropic medium approximation (3A) is usually preferable due to its conservative nature [7], similarly to the finite volume approximation used in Eq. 2. Finite difference approximation (3B) is also conservative and satisfies the grid maximum principle under some conditions [7,8]. Finite difference approximation (3C) is a simple modification of scheme (3A) with some averaging of the coefficients similar to approximation (2). Scheme (3D) is a generalization for the inhomoheneous case of the typical four-points approximation of mixed derivatives with constant coefficients. Finally, Finite difference approximation (3E) is a conservative scheme with an additional important property in comparison with (3A-3D): It uses the same stencil nodes for diagonal and off – diagonal conductivity tensor components. This property makes approximation (3E) more stable and ensures the positive definite property of the resulting tensor approximation on the local scale for piece-wise inhomogeneous anisotropic media which are typical for the multi-shell EEG/MEG/EIT forward models. Approximation of type 3(C) is the simplest one and not conservative. For all cases under consideration, the discretized problem is reduced to solving a large system of Linear Algebraic Equations (LAE) with a square 19- diagonal matrix (Fig. 2) of dimension $N_xN_yN_z$, and iterative methods are the best option of choice to deal with such systems of LAE.

As one of the simplest form of preconditioning almost not requiring additional computations one can suggest the Jacobi (diagonal) preconditioner type [12]. It allows to reduce a number of iterations in PDEs with strongly inhomogenious coefficients like in the Derichlet problem in the fictitious domain we are dealing here. However, the Jacobi preconditioner does not damp the increase in a number of iterations with the increase of a grid resolution. In addition to the Jacobi preconditioner, one can use as a preconditioner the system matrix corresponding to the case of the homogeneous isotropic limit. Because the Fast Fourier Transform (FFT) can be utilized to compute an inverse matrix of such a preconditioner, such kind of preconditioners is referred to as the *Fourier preconditioner* [11,14]. Along with image reconstruction problems, the Fourier preconditioner is successfully used in numerical analysis of PDEs [11-14] including the Poisson Equation in EIT/EEG [16]. In many cases, the Fourier preconditioner allows to eliminate dependence of an iteration number to convergence from

the grid resolution, as in case of the multigrid preconditioner [17]. We have checked efficiency of the mentioned types of preconditioned iterative methods using their standard realization in Matlab [18]. Taking into account the Dirichlet boundary conditions we have modified the module of postprocessing for the Fourier preconditioner by use of the sin-Fourier transform.

3 Validation and Numerical Examples

Numerical modeling of smooth analytic probe solutions for the Dirichlet problem has proved to be of the second order of approximation in regards of the grid step for all three approximations of mixed derivatives (3a), (3b) and (3c) .We have also validated the numerical methods against the analytics in the layered anisotropic spherical model [3]. Based on these simulation tests we have derived the performance figures for suggested numerical method. We have considered the popular in EEG 4-shell spherical model with the external radii of shells (in m) : R_1=0.084; R_2=0.065; R_3=0.05; R_4=0.03 and conductivities of shells (S/m) : σ_1 = 0.44; σ_2 = 0.02; σ_3 = 1.8; σ_4 = 0.25 correspondingly. The second outer shell modeling skull was assumed to be anisotropic with the tangential to radial conductivities ratio $\sigma_{2\tau}/\sigma_{2R}$=10. The transformation from the local spherical coordinate system to the global Cartesian system was performed for each skull layer voxel according to :

$$\sigma_2 = A^T \sigma_2^* A ,$$

where σ_2* is a diogonal conductivity tensor with eigenvalues ($\sigma_{2\tau}$, σ_{2R} , σ_{2R}) and A is a rotation matrix. The conductivity tensor in such a model of anisotropy is a fair approximation of the cranial plates conductivity in the human head [3]. The anisotropic spherical head was embedded into the fictitious cubic computational domain with the edge length of 0.1 m padded with dielectric media (air) with the conductivity of 10^{-10} S/m. The resulted computed topography is shown in Fig 3 for a source – sink pair, placed on the equator in the middle of the outer shell. In the bottom of Fig. 3 the simulated topography is compared with an approximate analytical solution [19]. The results show good agreement of the numerical solution with the analytics with some perceptible deviations near the dipole source, where it might be expected due to difference in discrete and analytical current source approximations.

To study the performance of the suggested method we have investigated dependence of the convergence rate from the grid resolution and the type of finite difference approximation. The number of iterations and the total computation time required to reach the given accuracy as a function of grid node number is shown in Fig. 4 and 5. For the smooth Dirichlet type solutions the BiCG method with the Jacobi-Fourier preconditioner requires not more than 10 iterations independently from the grid resolution and outperforms by a large factor the BiCG method with and without the Jacobi preconditioner in terms of the computational time. The number of iterations to convergence is about the same for all five mixed derivatives approximations (3A-3E) in all three preconditioned BiCG methods.

When the piece-wise 4-shell spherical model was used , the more stable results were obtained with approximation type (3B) , while approximation (3A) shows increase of iteration number in the BiCG JF method by factor of 2. The benefits of using the BiCG JF method are best pronounced for the 2 mm resolution and higher. For instance, to reach the accuracy of $\varepsilon=10^{-5}$ the required iteration number is not larger than 30 and does not depend on the grid resolution.

We have also tested our solver on the realistic MRI/CT based human head multishell model with the metal surgical clips in skull (shaped as a Greek letter "Π" with dimensions 12 mm x 12 mm x 12 mm, a crossection of 2 mm x 4 mm, and titanium conductivity 2.5e6 S/m,) as it shown in Fig. 6 and brain white matter conductivity tensor inferred from DTI (Fig. 7 and 8).

4 Discussion

We have presented a novel type of an EEG/EIT anisotropic FDM forward solver from the CG methods family . The combined Jacoby-Fourier preconditioner shows unprecedented performance and robustness. It is capable to solve 128x128x128 voxels anisotropic problems with eigenvalues ratio 10 : 1 and isotropic heterogeneity ratio 2.5e6 : 1 (explicit titanium clips modeling) within a minute runtime in the Matlab implementation. More importantly for EEG and EIT applications, our simulation results show that isotropic brain white matter versus anisotropic one introduces an error of up to 25 % for lead fields on scalp.

Acknowledgments

We acknowledge the contribution of Dr. David Hammond who helped with co-registration of the brain white matter DTI data to the T1 MRI image volume in line with his methods [22, 23].

References

1. Arridge, S.R.: Optical tomography in medical imaging. Inverse Problems, 15 (1999) R41-R93.
2. Gulrajani, R.M.: Bioelectricity and Biomagnetism. John Wiley & Sons, New York (1998).
3. Hallez, H., et. al.: Review on solving the forward problem in EEG source analysis. Journal of Neuroengineering and Rehabilitation. 4;46 (2007).
4. General-purpose computation using graphics hardware, http://www.gpgpu.org/.
5. Qin, C., Kang, N., Cao, N.: Performance evaluation of anisotropic diffusion simulation based tractography on phantom images. ACMSE 2007, March 23-24, 2007, Winston-Salem, NC, USA.
6. Salman, A., Turovets, S., Malony, A., Volkov, V.: Multi-cluster, mix-mode computational modeling of human head conductivity. IWOMP 2005/2006. LNCS 4315 (2008) 119-130.
7. Samarskii, A. A. "Theory of finite difference schemes." (1989).
8. Rybak, I. V. "Monotone and conservative difference schemes for elliptic equations with mixed derivatives 1." *Mathematical Modelling and Analysis* 9.2 (2004): 169-178.
9. Abrashin, V.N., Egorov, A.A., Zhadaeva, N.G. On a class of additive iterative methods. Differential Equations, 37,(2001) 1751-1760.
10. LeVeque, R.: Finite Volume Methods for Hyperbolic Problems, Cambridge University Press (2002).
11. Press, W.H., Teukolsky, S.A., Vetterling, W.T., Flannery, B.P.: The Numerical Recipes in C: The art of Scientific Computing. 2nd edition. Cambridge University Press, New York (1992).
12. Barrett, R., Berry, M., Chan, T. F. et al.: Templates for the Solution of Linear Systems: Building Blocks for Iterative Methods, SIAM, Philadelphia (1994)

13. Freund, R. and Nachtigal, N.: QMR: A quasi-minimal residual method for non-hermitian linear systems. Numer. Math. 60 (1991) 315-339.
14. Glowinski, R., Pan, T. W., & Periaux, J. (1994). A fictitious domain method for Dirichlet problem and applications. Computer Methods in Applied Mechanics and Engineering, 111(3), 283-303.
15. Van der Vorst, H.A., "BI-CGSTAB: A fast and smoothly converging variant of BI-CG for the solution of nonsymmetric linear systems," SIAM J. Sci. Stat. Comput., March 1992, Vol. 13, No. 2, pp. 631–644.
16. Volkov, V. M., Zherdetskij, A. A., Turovets, S. I., & Malony, A. D. (2010). A fast BiCG solver for the isotropic Poisson equation in the forward EIT problem in cylinder phantoms. Journal of Physics: Conference Series (Vol. 224, No. 1, p. 012153).
17. Hackbusch W. Multi-grid methods and applications. – Berlin : Springer-Verlag, 1985. – V. 4.
18. http://www.mathworks.com/help/matlab/ref/bicgstab.html
19. de Munck, D. J., & Peters, M. J. (1993). A fast method to compute the potential in the multisphere model. IEEE transactions on biomedical engineering, 40(11), 1166-1174.
20. Volkov, V.M., Zherdetskij, A.A., Turovets, S.I., & Malony, A.D. (2009). A 3D Vector-Additive Iterative Solver for the Anisotropic Inhomogeneous Poisson Equation in the Forward EEG problem". In Proceedings of ICCS 2009, G. Allen et al. (Eds.) ICCS 2009, Part I, LNCS 5544, pp. 511-520. Springer, Heidelberg (2009).
21. Ozog, D., Salman, A., Malony, A., Turovets, S., Volkov, V. and Tucker, D. Next-Generation Human Brain Neuroimaging and the Role of High-Performance Computing. The 2013 High Performance Computing & Simulation Conference (HPCS 2013) July 1 - 5, 2013, Helsinki, Finland.
22. Hammond, D.K., Scherrer, B. and Maloney, A .Incorporating anatomical connectivity into EEG source estimation via sparse approximation with corticalgraph wavelets.. IEEE International Conference onAcoustics, Signals and Signal Processing (ICASSP) 2012, Kyoto, Japan, March 2012.
23. Hammond, D.K., Scherrer, B., Warfield, S.K. Cortical graph smoothing : a novel method for exploiting DWI-derived anatomical brain connectivity to improve EEG source estimation. IEEE Trans Med Imaging, 2013, to appear.

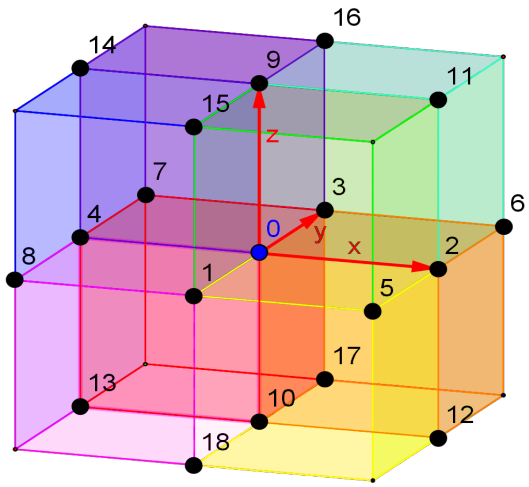

Fig. 1. The finite difference stencil of discrete approximation for the anisotropic problem

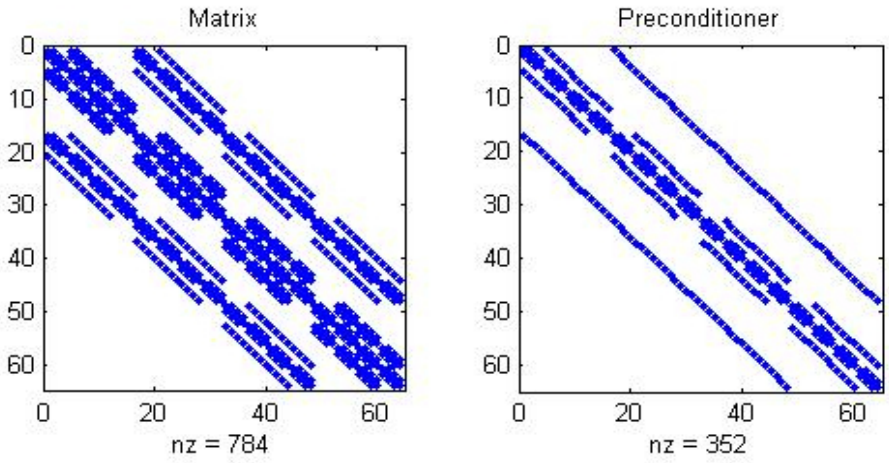

Fig. 2. Structure of the system matrix (left) and the preconditioner (right).

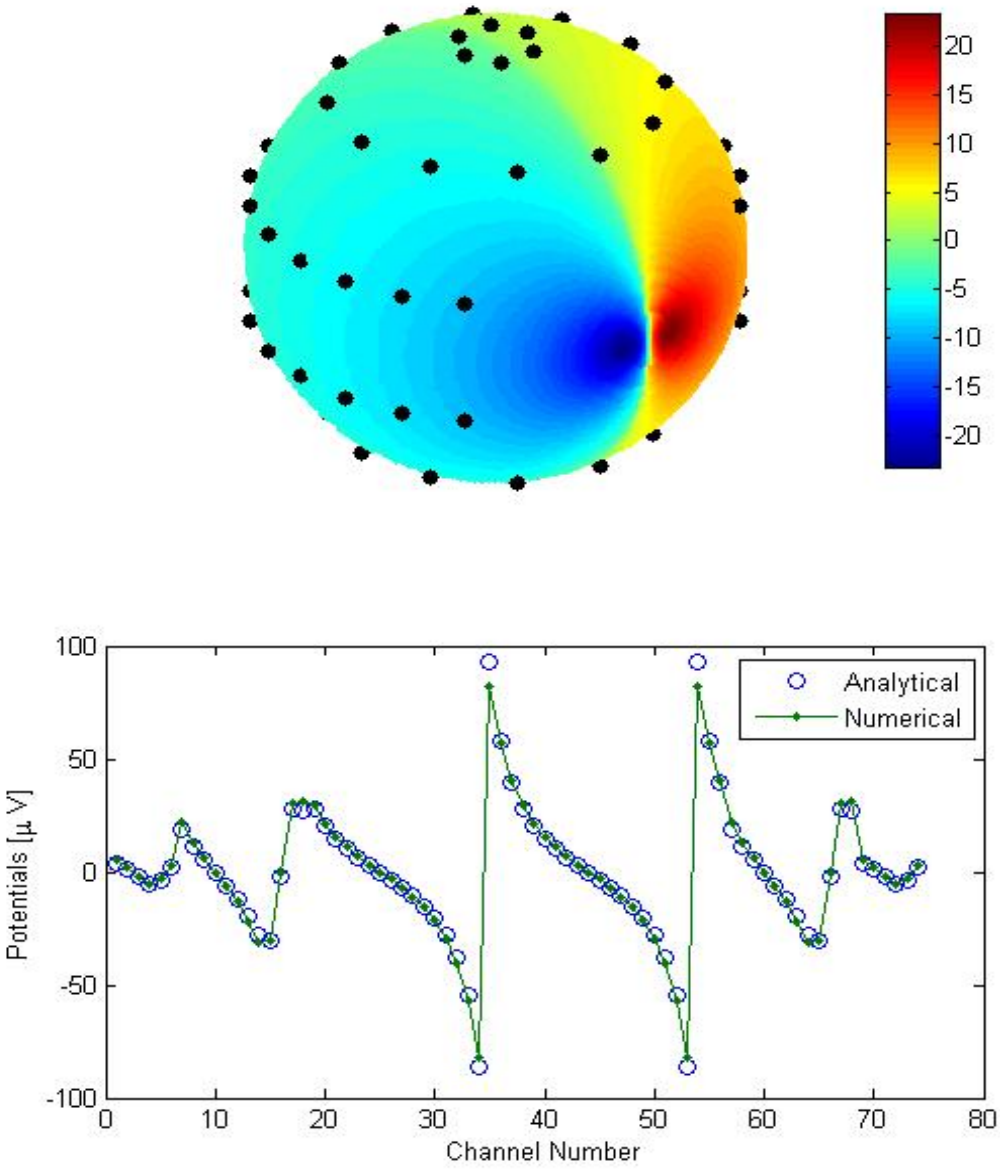

Fig. 3. Validation of the numerical scheme against the analytical solution in the anisotropic spherical model (de Munck and Peters, 1993) . The FD computed potentials (solid) and analytical (open circles) curves versus channel number. The 4-shell spherical model with R_1=0.084; R_2=0.065; R_3=0.05; R_4=0.03 [m] and σ_1 = 0.44; σ_2 = 0.02; σ_3 = 1.8; σ_4 = 0.25 [S/m] , $\sigma_{2\tau}/\sigma_{2R}$=10.

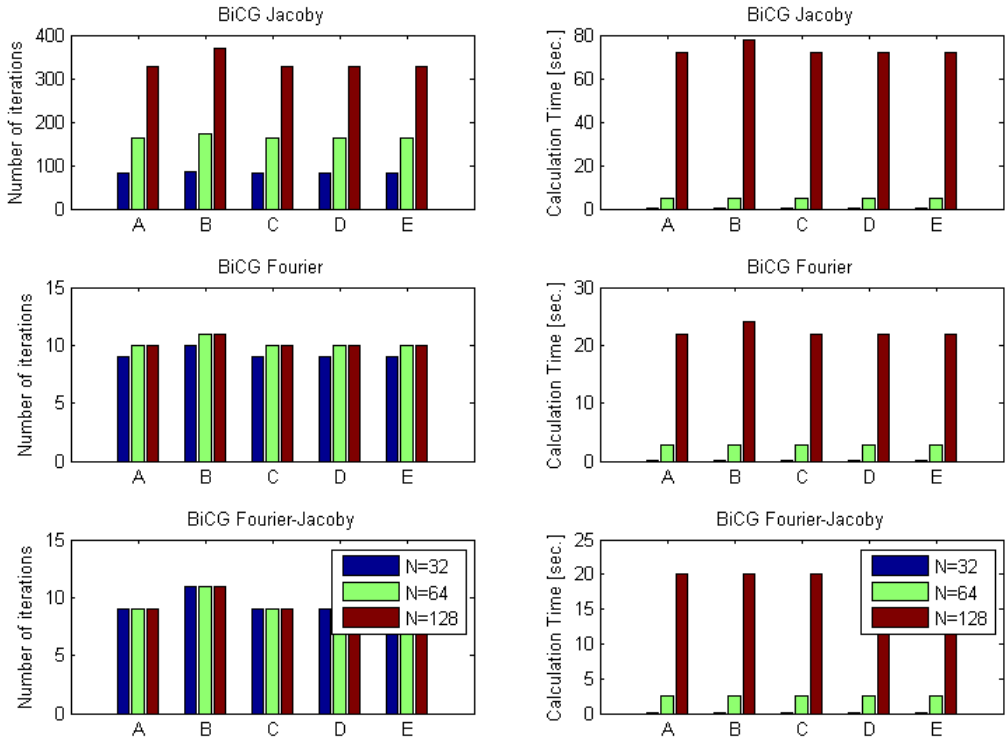

Fig. 4. Efficiency of different preconditioners for inhomogeneous smooth solutions (an analytical probe function) . Number of iterations (left) and runtime in seconds (right) versus a mixed derivative approximation type for different resolutions (N^3).

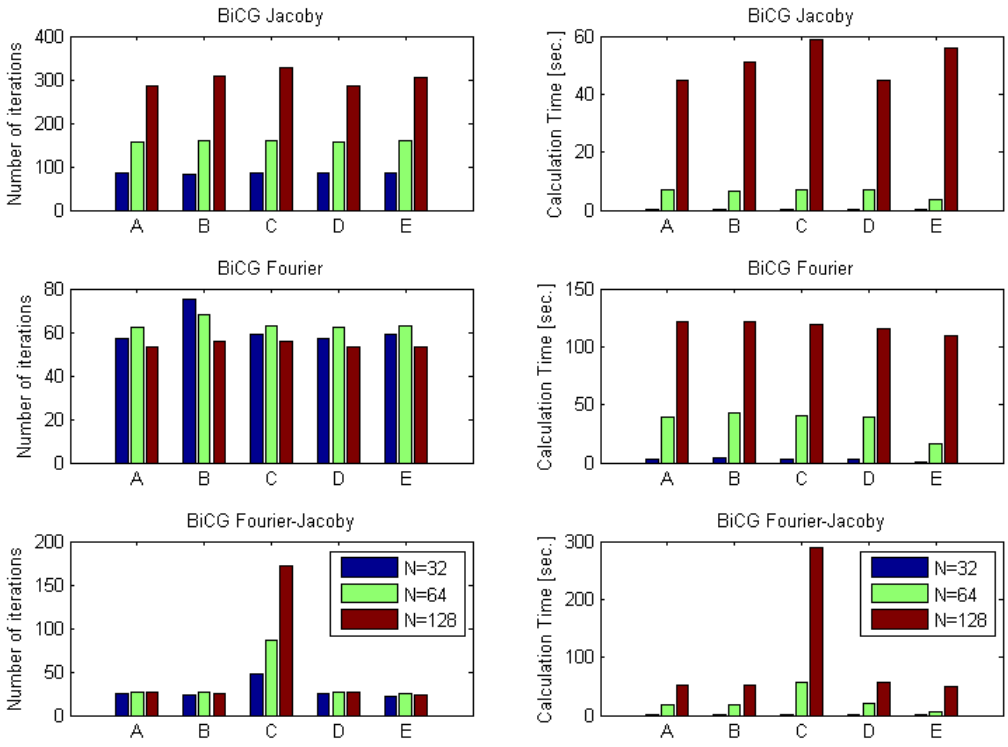

Fig. 5. Efficiency of different preconditioners for the piece-wise heterogeneous anisotropic spherical model (**cl. Fig. 3**). Number of iterations (left) and runtime in seconds (right) versus a mixed derivative approximation type for different resolutions (N^3). Approximation C is worse than others.

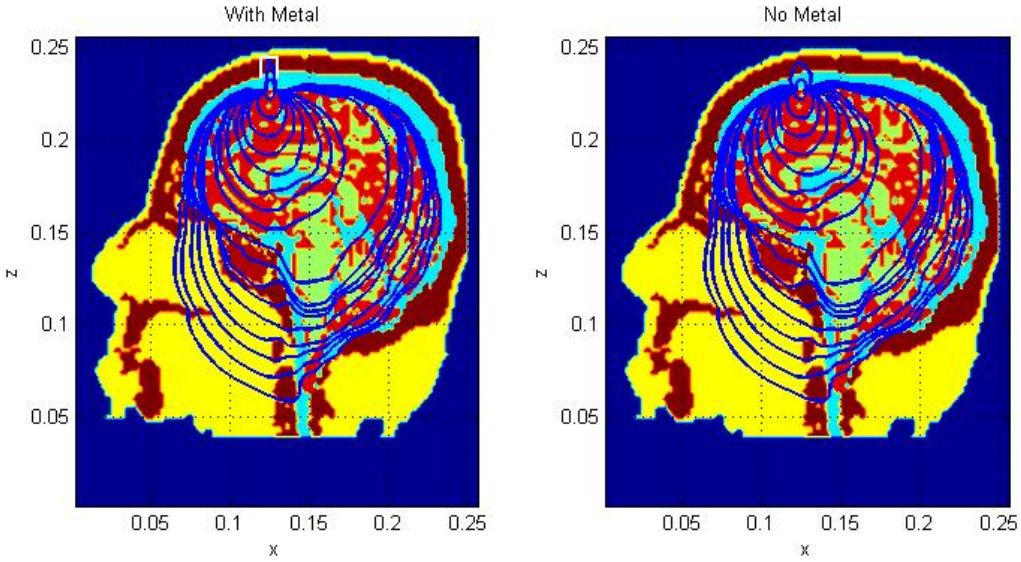

Fig. 6a. Modeling of impact of the titanium surgical clip (the white «pi») on the EEG forward solution in a "virtual" post-operational patient. A horizontally oriented dipole is of 0.6 cm from the clip . The shunting effect is getting more pronounced with the closer distance between the dipole and the clip and parallel orientation as it can be seen through the distortion of current stream lines.

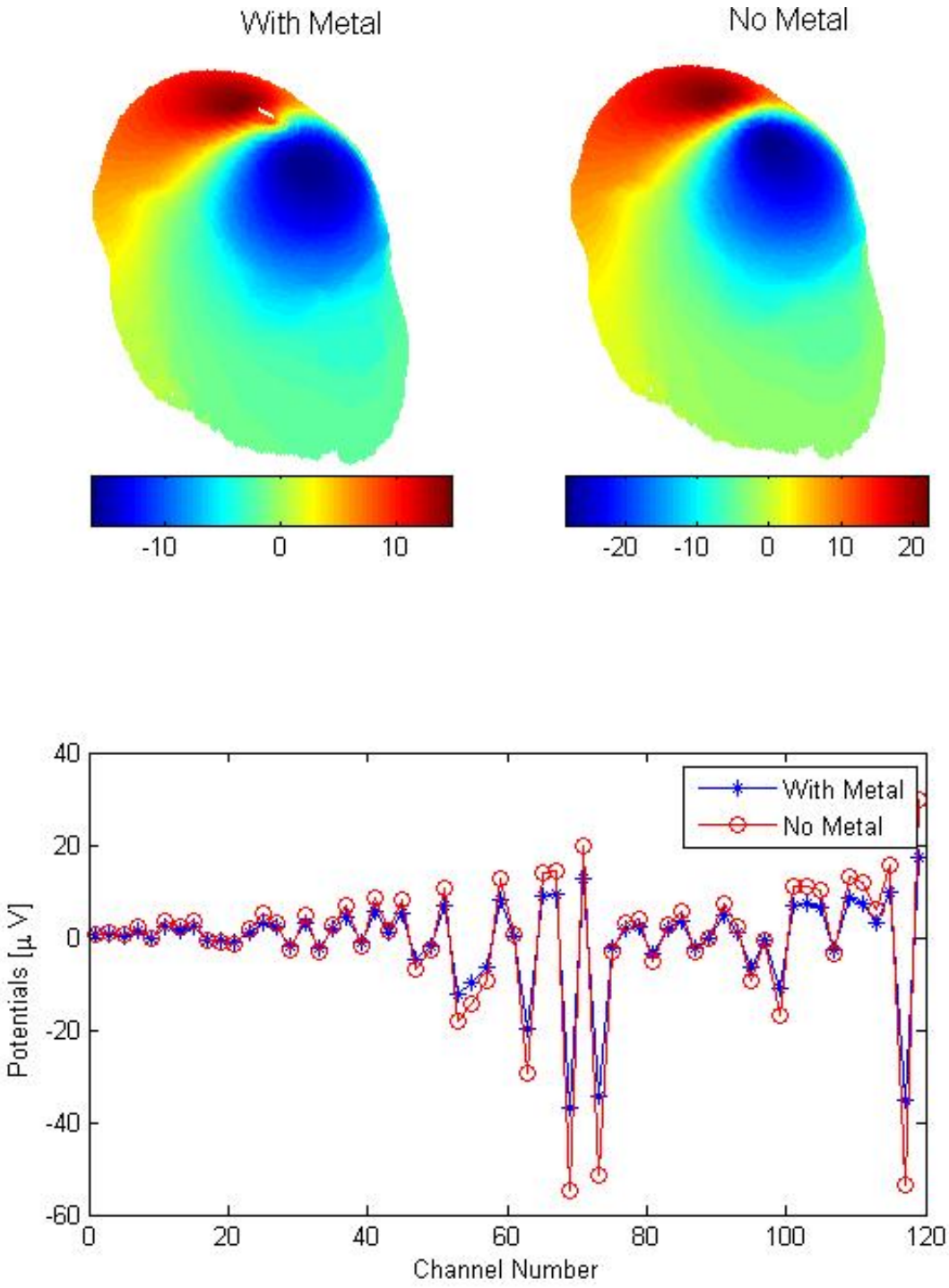

Fig. 6b. Impact of titanium surgical clip (the white «pi») on the EEG forward solution in post-operational patients. A horizontally oriented dipole is of 4 cm from the clip (left column) and 2 cm (right). The shunting effect is getting more pronounced with the closer distance between the dipole and the clip and parallel orientation as it can be seen through the distortion of equipotential lines.

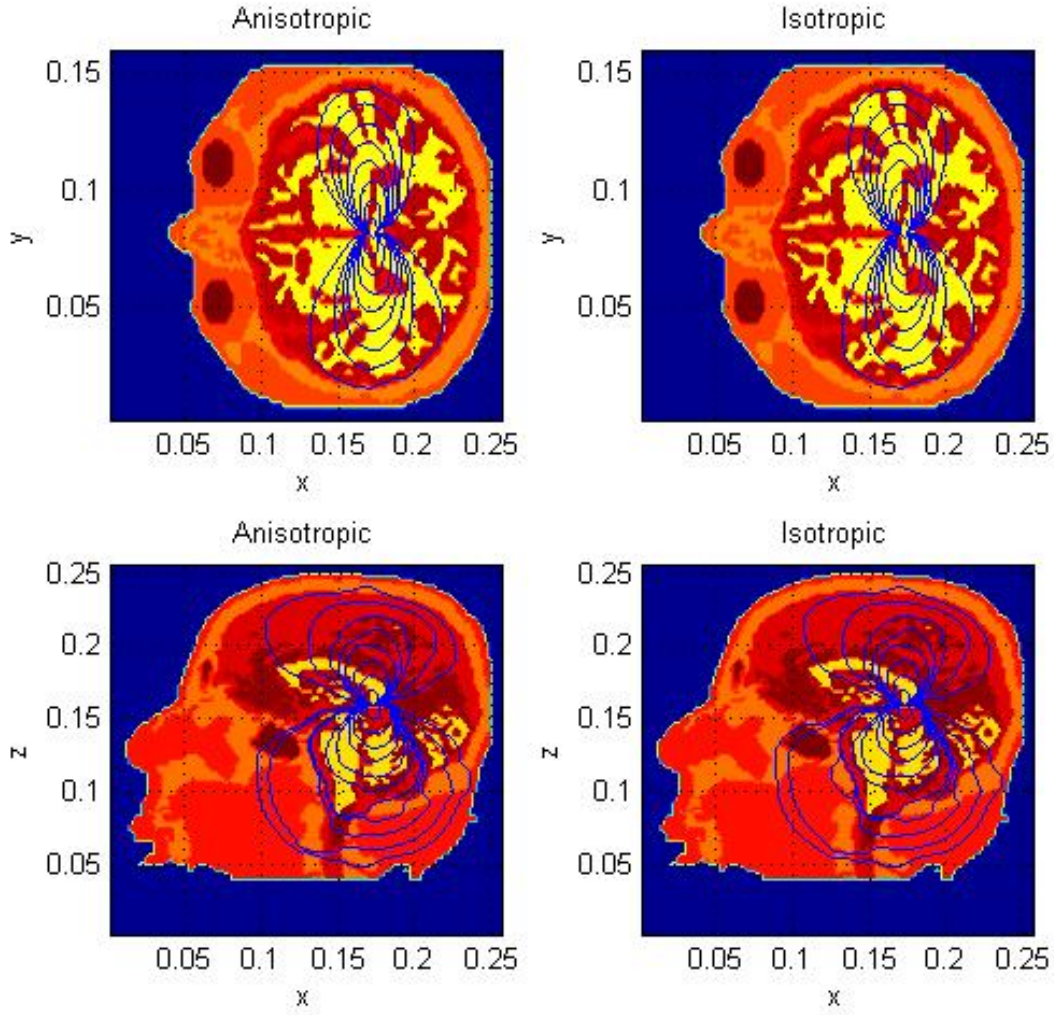

Fig. 7. Impact of brain white matter anisotropy on the EEG forward solution . A horizontally oriented dipole is placed deep in the central brain region. The distortion of current streamlines can be seen in the anisotropic case (left) relatively to the isotropic case (right).

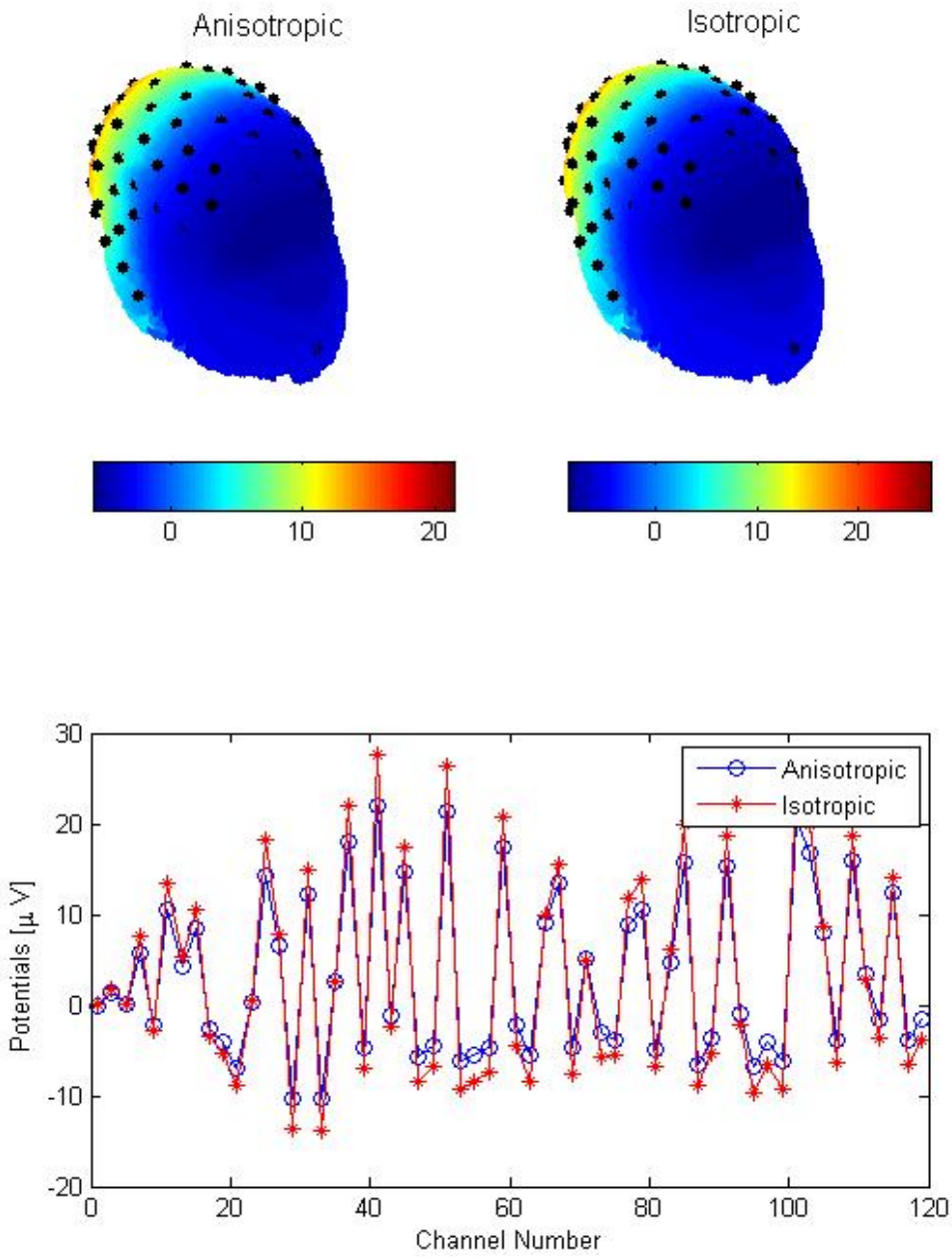

Fig. 8. Impact of brain white matter anisotropy on the EEG forward solution : 3D topography view (top) and 1D Voltages (μV) versus Channel Number detailed quantitative comparison (bottom) . A horizontally oriented dipole is placed deep in the central brain region.